frontiers in Marine Science

ORIGINAL RESEARCH
published: 23 May 2017
doi: 10.3389/fmars.2017.00152

Fixed-Nitrogen Loss Associated with Sinking Zooplankton Carcasses in a Coastal Oxygen Minimum Zone (Golfo Dulce, Costa Rica)

Peter Stief[1], Ann Sofie B. Lundgaard[1], Álvaro Morales-Ramírez[2], Bo Thamdrup[1] and Ronnie N. Glud[1, 3, 4]*

[1] Nordcee, Department of Biology, University of Southern Denmark, Odense, Denmark, [2] CIMAR, Universidad de Costa Rica, San José, Costa Rica, [3] Scottish Marine Institute, Scottish Association for Marine Science, Oban, United Kingdom, [4] Department of Ocean and Environmental Sciences, Tokyo University of Marine Science and Technology, Tokyo, Japan

Oxygen minimum zones (OMZs) in the ocean are of key importance for pelagic fixed-nitrogen loss (N-loss) through microbial denitrification and anaerobic ammonium oxidation (anammox). Recent studies document that zooplankton is surprisingly abundant in and around OMZs and that the microbial community associated with carcasses of a large copepod species mediates denitrification. Here, we investigate the complex N-cycling associated with sinking zooplankton carcasses exposed to the steep O_2 gradient in a coastal OMZ (Golfo Dulce, Costa Rica). ^{15}N-stable-isotope enrichment experiments revealed that the carcasses of abundant copepods and ostracods provide anoxic microbial hotspots in the pelagic zone by hosting intense anaerobic N-cycle activities even in the presence of ambient O_2. Carcass-associated anaerobic N-cycling was clearly dominated by dissimilatory nitrate reduction to ammonium (DNRA) at up to 30.8 nmol NH_4^+ individual^{-1} d^{-1}, followed by denitrification (up to 10.8 nmol N_2-N individual^{-1} d^{-1}), anammox (up to 1.6 nmol N_2-N individual^{-1} d^{-1}), and N_2O production (up to 1.2 nmol N_2O-N individual^{-1} d^{-1}). In contrast, anaerobic N-cycling mediated by free-living bacteria proceeded mainly through anammox and denitrification in the anoxic bottom water, which underpins the distinctive microbial metabolism associated with zooplankton carcasses. Pelagic N-loss is potentially enhanced by zooplankton carcasses both directly through N_2 and N_2O production, and indirectly through NH_4^+ production that may fuel free-living anammox bacteria. We estimate that in the hypoxic water layer of Golfo Dulce, carcass-associated N_2 and N_2O production enhance N-loss as much as 1.4-fold at a relative carcass abundance of 36%. In the anoxic bottom water, however, N-loss is likely enhanced only marginally due to high ambient rates and low zooplankton abundance. Thus, zooplankton carcasses may enhance N-loss mainly at the hypoxic boundaries of OMZs which are usually more extensive in open-ocean than in coastal settings. Notably, these contributions by zooplankton carcasses to pelagic N-loss remain undetected by conventional, incubation-based rate measurements.

Keywords: animal-microbe interactions, copepods, ostracods, carcasses, oxygen minimum zone, nitrogen cycle, fixed-nitrogen loss, ^{15}N-stable isotope labeling

OPEN ACCESS

Edited by:
Tim Kalvelage, ETH Zurich, Switzerland

Reviewed by:
Rainer Kiko, GEOMAR Helmholtz Centre for Ocean Research Kiel (HZ), Germany
Annie Bourbonnais, University of Massachusetts Dartmouth, United States

****Correspondence:***
Peter Stief
peterstief@biology.sdu.dk

Specialty section:
This article was submitted to Marine Biogeochemistry, a section of the journal Frontiers in Marine Science

Received: *30 November 2016*
Accepted: *05 May 2017*
Published: *23 May 2017*

Citation:
Stief P, Lundgaard ASB, Morales-Ramírez Á, Thamdrup B and Glud RN (2017) Fixed-Nitrogen Loss Associated with Sinking Zooplankton Carcasses in a Coastal Oxygen Minimum Zone (Golfo Dulce, Costa Rica). Front. Mar. Sci. 4:152. doi: 10.3389/fmars.2017.00152

INTRODUCTION

Marine mesozooplankton, commonly dominated by copepods, is increasingly recognized to host unique microenvironments in the pelagic macroenvironment (Tang et al., 2010). Copepod guts are oxygen-depleted and low in pH (Tang et al., 2011; Glud et al., 2015), which is remarkable considering their small size and the high ambient oxygen and pH levels. Anoxic guts have otherwise been reported for much larger benthic invertebrates that are exposed to low ambient oxygen levels in sediments (Plante and Jumars, 1992; Stief and Eller, 2006; Stief et al., 2009). Additionally, copepods and their carcasses constitute local sources of particulate and dissolved organic matter and nutrients, which attracts and feeds free-living and animal-associated bacteria (Steinberg et al., 2000; Tang et al., 2006; Saba et al., 2011). Thus, in pelagic ecosystems, copepods and other mesozooplankton represent vastly abundant "microbial hotspots" with unique biogeochemical features (Tang, 2005; Tang et al., 2010; Nuester et al., 2014). In this sense, zooplankters, and in particular their carcasses, resemble sinking phytodetritus aggregates that host dense microbial communities within a low-oxygen microenvironment (Ploug et al., 1997; Glud et al., 2015; Klawonn et al., 2015; Stief et al., 2016). The presence of zooplankton carcasses in the water column results from non-consumptive mortality, caused by e.g., parasitism or turbulences, which allows extensive microbial degradation of carcasses during their descent to the seabed (Tang et al., 2011). Estimates of the relative abundance of zooplankton carcasses have lately been improved with new staining techniques (Bickel et al., 2009; Elliott and Tang, 2009), which revealed surprisingly high carcass abundances in natural settings, often in the order of 10–30% of the total zooplankton population (Tang et al., 2009, 2014). For marine habitats of tropical and subtropical regions, relative carcass abundances as high as 20–70% (Tang et al., 2009) and 10–90% (Elliott and Tang, 2009) are reported.

Recent investigations into copepod microbiomes have revealed a number of recurring bacterial groups, such as *Vibrio* sp., Bacteroidetes, Firmicutes, Actinobacteria, and *Pseudoalteromonas* sp., that are associated with different copepod species from different ecosystems (Gerdts et al., 2013; De Corte et al., 2014; Moisander et al., 2015; Scavotto et al., 2015; Shoemaker and Moisander, 2015). Separating out the microbial communities that colonize the gut or the exoskeleton of zooplankton is challenging though (Møller et al., 2007; De Corte et al., 2014; Skovgaard et al., 2015). Additionally, the metabolic functions of zooplankton-associated bacteria remain largely unknown, unlike those of microorganisms associated with benthic invertebrates (Dubilier et al., 2001; Martinez-Garcia et al., 2008; Hoffmann et al., 2009; Stief et al., 2009). Notable exceptions are the associations between copepods and N_2-fixing and denitrifying bacteria (Zehr et al., 1998; Glud et al., 2015; Scavotto et al., 2015).

Denitrification activity in carcasses of the relatively large copepod *Calanus finmarchicus* is most pronounced at low ambient O_2 levels (Glud et al., 2015). Evidence is rapidly accumulating that copepods and other mesozooplankton are indeed abundant in and around oceanic oxygen minimum zones (OMZs) (Escribano et al., 2009; Teuber et al., 2013; Wishner et al., 2013; Hirche et al., 2014; Parris et al., 2014). Also the microbial communities associated with copepod carcasses, including those attached to the exoskeleton, are exposed to the low ambient O_2 levels and will likely respond with increased rates of anaerobic metabolism. This will reinforce the functioning of zooplankton carcasses as O_2-depleted, pelagic hotspots with possible large-scale biogeochemical implications. Globally, OMZs are responsible for up to 50% of the oceanic fixed-nitrogen loss (N-loss) via denitrification and anammox (DeVries et al.,, 2013). Copepod carcasses may directly contribute to this N-loss via denitrification and possibly anammox (Glud et al., 2015). Model results further suggest that migrating zooplankton actively transports organically bound nitrogen to depth where it is partially released as NH_4^+ and may fuel free-living anammox bacteria and thus contribute indirectly to pelagic N-loss (Bianchi et al., 2014). The quantitative importance of this pathway was recently challenged though because zooplankton may down-regulate NH_4^+ excretion upon exposure to extreme hypoxia or anoxia (Kiko et al., 2016).

Here, we measured diverse microbial N-cycle activities directly associated with the carcasses of abundant groups of zooplankton in a temperature-stratified coastal basin with anoxic bottom water (Golfo Dulce, Costa Rica). This coastal marine OMZ is an environmental showcase for pelagic N-loss through anammox and denitrification activity (Dalsgaard et al., 2003). Copepod and ostracod carcasses were incubated in seawater sampled from three water layers in which different temperature and O_2 conditions prevail. The seawater was amended with $^{15}NO_2^-$ to quantify both aerobic and anaerobic pathways of the microbial N-cycle. The basic hypothesis was that zooplankton carcasses represent anoxic microsites at which anaerobic N-cycling can take place. The ultimate goal was to assess the quantitative contribution by zooplankton carcasses to N-loss in a coastal OMZ, which would not be captured by conventional, incubation-based techniques to measure rates of pelagic N-cycling.

MATERIALS AND METHODS

Study Site and Sample Collection

Zooplankton and water samples were collected at the northern end of Golfo Dulce (08°41′60″N, 83°23′24″W) which corresponds approximately to Station 1 in a previous study (Ferdelman et al., 2006; **Figure 1A**). This coastal marine basin is up to 215 m deep and characterized by a temperature-stratified water column and anoxic bottom water with high anammox activity (Thamdrup et al., 1996; Dalsgaard et al., 2003; Ferdelman et al., 2006; Morales-Ramírez et al., 2015). All samplings were made at the same time of day (11 am–1 pm) during a 1-week field campaign in January 2015.

Zooplankton for ^{15}N-incubation experiments was sampled on three occasions by hauling the 0–40 m depth interval with a conical net (0.5 m in diameter, 100 μm mesh size). The catch of 1–2 hauls was kept in 10 L of oxygenated seawater collected at 20 m depth with Niskin bottles and transported to the

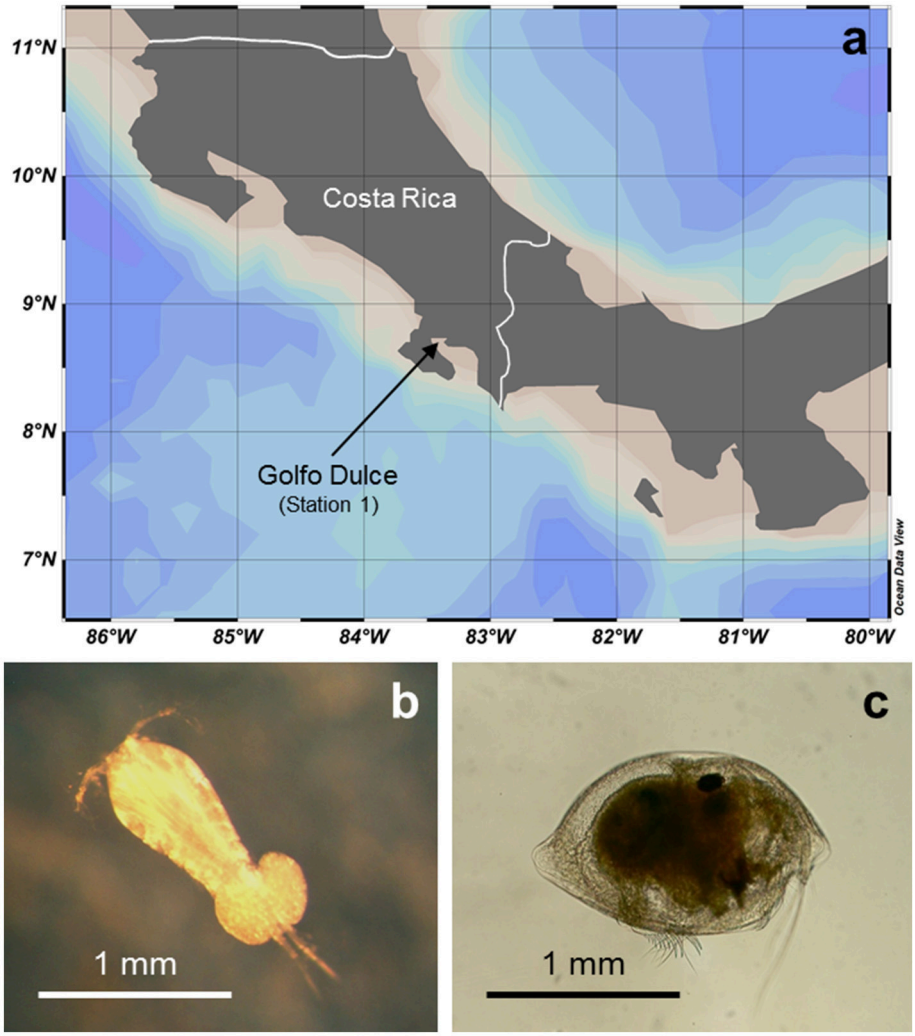

FIGURE 1 | Study site and representative zooplankton. (a) Geographical location of Golfo Dulce (GD) at the Pacific coast of Costa Rica; the tip of the arrow points to the targeted sampling station. **(b)** *Oncaea* sp., the most abundant copepod and **(c)** *Cypridina* sp., the most abundant ostracod in GD at the time of the current study. See Table S2 for detailed list of identified taxa.

laboratory within 1 h. Zooplankton for community analysis was collected on three occasions from three discrete depth intervals (0–40, 40–70, and 70–100 m) using the same net equipped with a remotely controlled closing device. These zooplankton samples were immediately preserved with formaldehyde (4% final concentration) for later taxonomic determination. Seawater for ^{15}N-incubation experiments was collected at approximately the center of the depth intervals for which the zooplankton community analyses were made (i.e., 20, 60, and 90 m).

Multiple water column profiles of O_2 concentration and temperature were measured during the time period in which zooplankton and seawater were sampled, using a CTD (Sea & Sun Technology) equipped with an O_2 microsensor (Revsbech, 1989).

Zooplankton Community Analysis

Zooplankton samples from the three depth intervals were aliquoted with a Folsom plankton splitter, identified to genus or species level, and counted in a Bogorov chamber. For the different samples, the aliquot size was varied between 1/8 and 1/32 to arrive at a minimum count of 200 individuals. Based on these counts and the water volume cleared with the vertical hauls, the *in situ* abundances of the different zooplankton taxa were calculated.

^{15}N-Stable-Isotope Incubations

Microbial N-transformations associated with zooplankton carcasses were measured for copepods and ostracods as the two taxonomic groups of zooplankton that were abundant in all samples. Carcasses were incubated in seawater from three water layers adjusted to the respective *in situ* temperature and O_2 conditions [i.e., upper water layer: 26°C/100% air saturation (AS), intermediate water layer: 21.5°C/0–25% AS, and lower water layer: 17°C/0% AS] (Table S1). The resulting six combinations of zooplankton incubations were compared to

the respective seawater incubations. Each of these combinations was run in 3–5 replicates in 100-μm-filtered seawater (i.e., in the presence of free-living bacteria), while 1 additional replicate was run in 0.2-μm-filtered seawater (i.e., in the absence of free-living bacteria).

On the day of collection, the zooplankton samples were screened for dead copepods and dead ostracods. Depending on availability, 25–50 copepod and ostracod carcasses were carefully transferred into replicate 20-mL vials filled with 100-μm-filtered seawater from the respective water layer. The copepod community comprised various species (Table S2) and care was taken that every vial contained carcasses representing most of the copepod diversity. In contrast, the ostracod community comprised only one species (Table S2). Dry weight and carbon and nitrogen contents of copepod and ostracod carcasses were obtained for 4 separately collected batches of 25 individuals each. Carcasses were transferred onto pre-combusted glass fiber filters (GC50, Advantec), freeze-dried overnight, weighed, and analyzed on an elemental analyzer (Delta V Advantage, Thermo Scientific) against protein and acetanilide standards.

The aliquoted copepods and ostracods were pre-incubated overnight (12 h) in 100 μm-filtered seawater collected at the respective water depth adjusted to near-*in situ* temperature and O_2 conditions. This pre-incubation time was chosen to mimic the sinking of zooplankton carcasses through a 30–40 m depth interval (Kirillin et al., 2012) during which carcass degradation may be initiated. The ^{15}N-incubations were prepared on the next day using acid-washed, sample-rinsed glass bottles (25 mL) equipped with optode spots for contactless O_2 measurements (PyroScience, Germany) and sealed with butyl stoppers to enable sample extraction. Preparation, incubation, and sampling of the glass bottles were made as described by Stief et al. (2016). Briefly, the bottles were filled with the appropriate mixture of oxygen- and helium-flushed seawater (for 15 min each) to arrive at the desired air saturation level of O_2. This degassing procedure increases the pH of seawater by <0.1 pH units, whereas it increases the pH of freshwater by ∼1 pH unit. ^{15}N-tracer was added as $Na^{15}NO_2$ (98 atom% ^{15}N; Sigma-Aldrich) at a final concentration of ∼3 μmol L^{-1}, which allowed to trace both aerobic and anaerobic pathways of the microbial N-cycle. *In situ* NO_2^- concentrations in GD were up to 0.72 μmol L^{-1} at the time of the current study (Padilla et al., 2017). The pre-incubated carcasses were added using a plastic pipette. The bottles were quickly sealed without entrapping gas bubbles and mounted on a plankton wheel at the respective temperature and in darkness. The rotation of the plankton wheel assured that the zooplankton carcasses remained continuously suspended. Oxygen measurements and water sampling were carried out every 2 h for a total of 8 h. Water sampling using two syringes (one for sample extraction and one for replacement of water) served also to maintain the ambient O_2 level within a reasonable range of variation. On the basis of the preceding O_2 measurement, the O_2 concentration in the replacement water was adjusted to a level that would compensate any observed concentration decrease. Oxygen consumption rates were calculated according to Stief et al. (2016).

Nitrogen Analyses

Each 3-mL water sample was split into 1.5 mL for N_2 and N_2O analyses and 1.5 mL for dissolved inorganic nitrogen (DIN) analyses. The N_2/N_2O sample was injected into a helium-flushed and half-evacuated 3-mL exetainer (Labco, U.K.) that contained 50 μL $ZnCl_2$ (50% w/v) for sample preservation. The DIN sample was immediately frozen at −20°C. Isotopically labeled dinitrogen (^{15}N-N_2) was analyzed in the headspace of exetainer samples on a gas chromatography-isotopic ratio mass spectrometer (Delta V Plus, Thermo Scientific) (Dalsgaard et al., 2012) with the excess above natural abundance calculated according to Nielsen (1992). Many samples taken at the first time point had higher N_2 concentrations than the consecutive samples, probably due to incomplete equilibration between the water phase and the gas present in tiny gas bubbles or within the butyl stoppers, and were thus excluded from rate calculations. Total nitrous oxide was analyzed in the same exetainers on a gas chromatograph (GC 7890, Agilent Technologies). ^{15}N-labeled NO_3^- (McIlvin and Altabet, 2005), NO_2^- (Füssel et al., 2012), and NH_4^+ (Warembourg, 1993) were analyzed with the cadmium reduction/sulfamic acid, sulfamic acid, and hypobromite assay, respectively, followed by ^{15}N-N_2 analysis on the gas chromatography-isotopic ratio mass spectrometer. The coefficients of variation of replicated $^{15}NO_3^-$, $^{15}NO_2^-$, and $^{15}NH_4^+$ standards (n = 7–10) amounted to 4, 5, and 6%, respectively. Total nitrate and nitrite were analyzed spectrophotometrically (Garcia-Robledo et al., 2014). Total ammonium was analyzed with the salicylate method (Bower and Holm-Hansen, 1980).

Rate Calculations

Turnover rates of N compounds (^{15}N-labeled and total N-pools) were calculated from linear concentration changes during the incubation period and corrected for the dilution due to repeated sampling (Stief et al., 2016). Rates determined in seawater incubations with seawater only were subtracted from those determined in zooplankton incubations to arrive at individual-specific process rates. The ^{15}N-turnover rates were used to calculate the process rates of NO_2^- oxidation, denitrification, and dissimilatory nitrate reduction to ammonium (DNRA): (a) NO_2^- oxidation rate equals $^{15}NO_3^-$ production rate divided by ^{15}N-labeling percentage (FN), (b) denitrification rate equals $^{30}N_2$ production rate divided by FN^2, and (c) DNRA rate equals $^{15}NH_4^+$ production rate divided by FN. For different processes and water depths, FN values of two different N-pools were considered: (a) for the NO_2^- oxidation rate and for the upper water layer, the measured ^{15}N-labeling percentage of the NO_2^- pool (FN_{NO2}) was used and (b) for denitrification and DNRA and for the intermediate and lower water layers, the measured ^{15}N-labeling percentage of the NO_x (i.e., $NO_3^- + NO_2^-$) pool (FN_{NOx}) was used. The latter option was chosen because in incubations with seawater from the intermediate and lower water layers, strong NO_3^- consumption accompanied $^{15}NO_2^-$ consumption, which diluted the ^{15}N-labeled NO_x pool. Nitrite produced by NO_3^- consumption may bypass the ambient NO_2^- pool and may be directly turned over in the denitrification and DNRA reactions (De Brabandere et al., 2014).

Anammox rates (AMX_{total}) were calculated as:

$$AMX_{total} = 1/FN_{NO2} \times (P_{29} + 2 \times (1 - 1/FN_{NO2}) \times P_{30}) \quad (1)$$

where P_{29} and P_{30} denote the production rates of single-labeled and double-labeled N_2, respectively (Thamdrup and Dalsgaard, 2002). This calculation neglects the contribution by anammox to $^{30}N_2$ production resulting from the accumulation of $^{15}NH_4^+$ through DNRA, which is justified because the ^{15}N-labeling percentage of the NH_4^+ pool remained ≤4% (Song et al., 2013). Previous studies found a tendency for anammox rates determined with $^{15}NO_2^-$ to be higher than rates determined with $^{15}NH_4^+$ (De Brabandere et al., 2014). In a comparison of anammox rates determined with either of the two labeled substrates during our expedition, the $^{15}NO_2^-$-based rates at 90 m, the only depth where we detected anammox, were only slightly (14%) higher than those based on $^{15}NH_4^+$ (Laura A. Bristow, pers. comm.). Thus, the potential bias resulting from the use of $^{15}NO_2^-$ in our study should not have any substantial impact on the results and conclusions.

In incubations with seawater from the intermediate water layer, high consumption rates of $NO_{3\ total}^-$ and $NH_{4\ total}^+$ reduced the net production rates of $^{15}NO_3^-$ and $^{15}NH_4^+$. The concentration time series of $^{15}NO_3^-$ and $^{15}NH_4^+$ were thus corrected to allow calculation of gross production rates:

$$C^{15}N_{t(i+1)corrected} = C^{15}N_{t(i+1)} - CN_{total\ t(i+1)}/CN_{total\ t(i)} \times C^{15}N_{t(i)} + C^{15}N_{t(i)corrected} \quad (2)$$

where C denotes concentrations of ^{15}N-labeled (^{15}N) or total N-pools (N_{total}) measured at time point $t_{(i)}$ or the following time point $t_{(i+1)}$.

Statistics

Linear regression analysis was used to test, if individual concentration time series had a slope significantly different from zero. The process rate derived from a concentration time series that did not meet this criterion was taken as zero. One-sample *t*-tests were used to test, if mean process rates were different from zero at a significance level of $p = 0.05$ (one-tailed). Grubbs' test for outliers was used to test, if incubations in 0.2-μm-filtered seawater had significantly lower process rates than incubations in 100-μm-filtered seawater. Student's *t*-tests were used to identify differences in individual-specific process rates between copepods and ostracods within a given water layer at a significance level of $p = 0.05$ (two-tailed). One-way ANOVA was used to identify differences in individual-specific process rates between the three water layers within a given taxonomic group of zooplankton at a significance level of $p = 0.05$ (two-tailed), followed by Holm-Sidak *post-hoc* tests. A non-parametric correlation analysis was conducted for N_2O production rates vs. turnover rates of other N-cycle processes.

RESULTS

Environmental Settings in Golfo Dulce

At the time of the study, the water column at the targeted station in Golfo Dulce (GD) was temperature-stratified with the thermocline located at ca. 30–50 m water depth (**Figure 2A**). The water column was further divided into an upper oxic, an intermediate hypoxic/anoxic, and a lower anoxic layer (**Figure 2B**). Oxygen concentrations were relatively stable directly at the surface and below 60 m water depth. In the depth interval 20–60 m, however, O_2 concentration showed large variations between the five sampling days. Additionally, rapid fluctuations between hypoxic and almost fully anoxic conditions were observed for individual sampling days on which O_2 profiles were repeated 2–3 times within a time period of 4 h.

Zooplankton abundance was high in the upper depth interval and progressively decreased to 10-fold lower levels in the lower depth interval (**Figure 2C**). The zooplankton community was dominated by small copepods making up ca. 50% of the total zooplankton abundance, whereas ostracod abundance was ca. 10-fold lower. The most common copepods were *Oncaea* sp., *Oithona* sp., and unidentified copepodites; the only ostracod identified was *Cypridina* sp. which had a similar body size as the most common copepods (**Figures 1B,C**; Table S2).

The copepod and ostracod carcasses used for incubation experiments had dry weights of 34.9 ± 7.8 and 61.3 ± 16.9 μg ind.$^{-1}$, respectively (mean ± standard deviation, $n = 4$ batches of 25 individuals each). The carbon contents were 20.4 ± 8.4 and 18.9 ± 5.1 μg ind.$^{-1}$ for copepod and ostracod carcasses, respectively; the nitrogen contents were 2.8 ± 0.6 and 3.2 ± 0.8 μg ind.$^{-1}$ for copepod and ostracod carcasses, respectively. The molar C/N ratios thus amounted to 8.2 ± 2.3 and 6.9 ± 0.2 for copepod and ostracod carcasses, respectively. The copepod and ostracod carcasses were not significantly different in any of these characteristics ($p > 0.05$, Student's *t*-test).

Oxygen Dynamics in Zooplankton and Seawater Incubations

Oxygen concentrations in zooplankton and seawater incubations were relatively stable for the oxic and anoxic water layer (Figures S1A,C). Strong fluctuations in O_2 concentration were observed in zooplankton incubations in water from the hypoxic/anoxic layer, with anoxic conditions occurring at three out of nine sampling time points (Figure S1B), which resembled the O_2 dynamics observed in the intermediate water layer in GD (**Figure 2B**).

Carcass-associated O_2 consumption rates (O_2-$Cons_{ZP}$) were always significantly different from zero and were not significantly different between copepods and ostracods within any given water layer (Figure S2a,e; Tables S3–S5). However, for both the copepod and the ostracod carcasses, O_2-$Cons_{ZP}$ rates were significantly higher in the hypoxic/anoxic than in the oxic water layer (Table S6).

Nitrogen Cycling Associated with Zooplankton Carcasses

Generally, zooplankton incubations in 0.2-μm-filtered seawater (white circles in **Figure 3**, Figures S2, S3) did not result in lower-end, statistical outliers ($p > 0.05$, Grubbs' test for $n = 72$ individual measurements), which suggests that the observed N-cycling in the zooplankton incubations was due

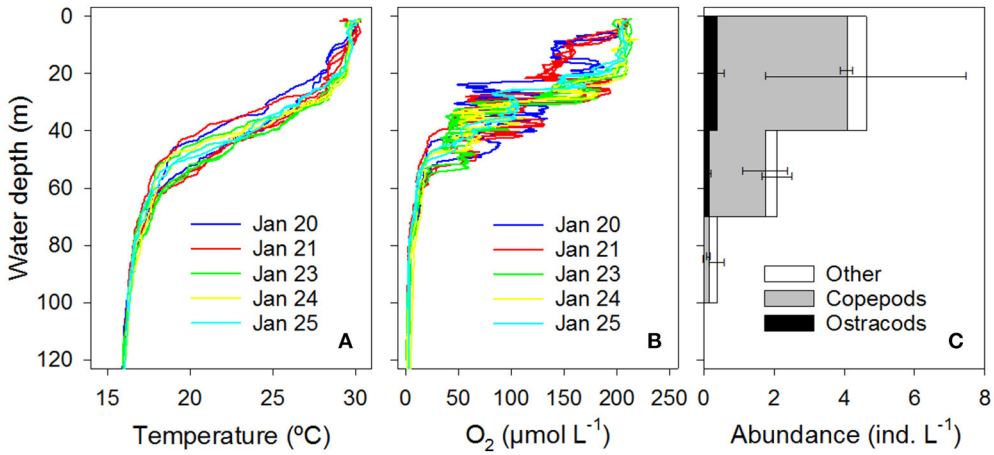

FIGURE 2 | Environmental settings in Golfo Dulce. Vertical gradients of **(A)** temperature and **(B)** O_2 concentration obtained from multiple CTD casts during the time of the current study; profiles shown in the same color were measured on the same day. **(C)** Vertical distribution of copepods, ostracods, and other mesozooplankton in three depth intervals in GD. Means and standard error of three samplings are shown. See Table S2 for detailed list of identified taxa.

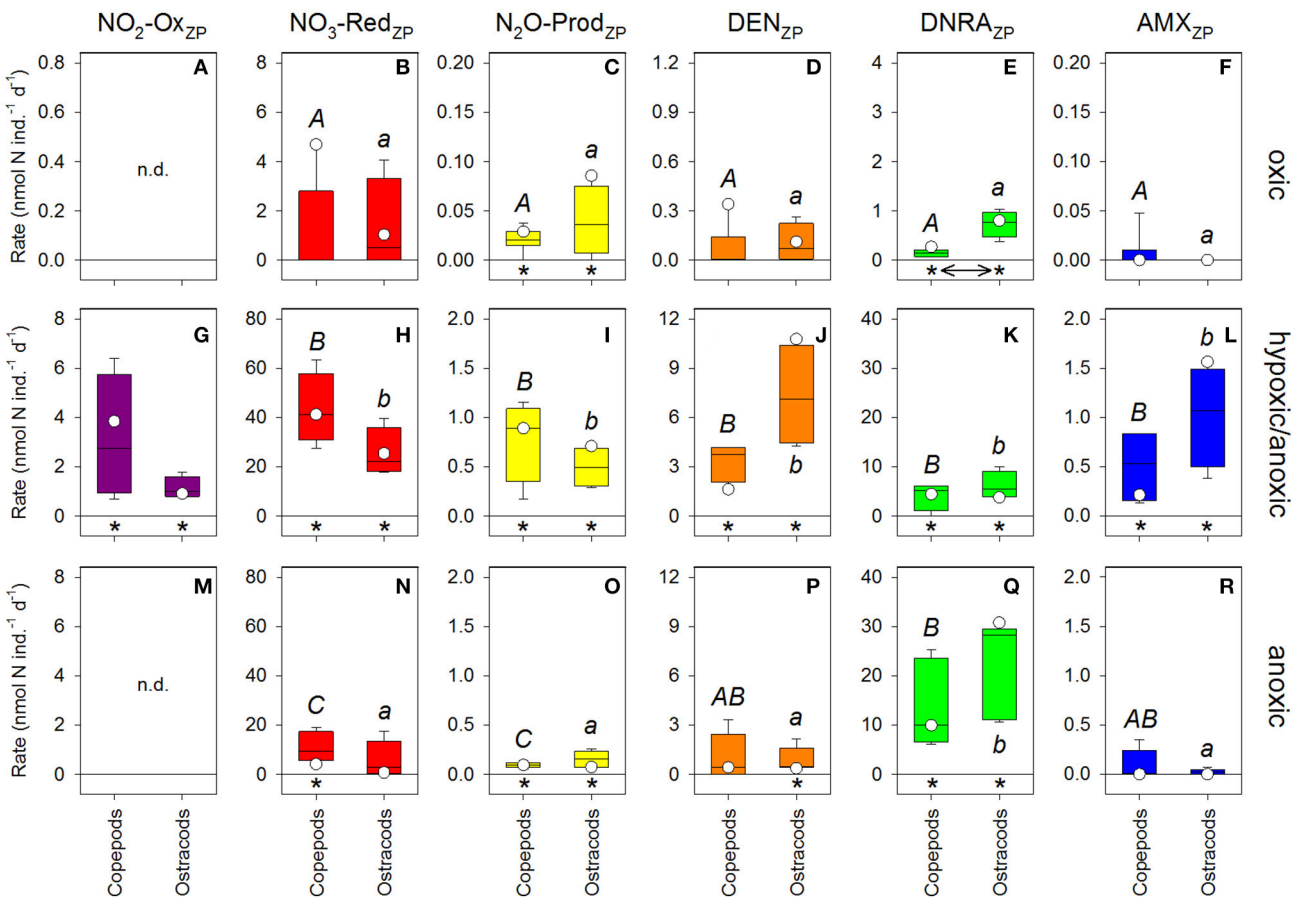

FIGURE 3 | Individual-specific N-cycling rates. Zooplankton carcasses were incubated in seawater collected in **(A–F)** oxic, **(G–L)** hypoxic/anoxic, and **(M–R)** anoxic layers in GD and maintained at near-*in situ* O_2 concentrations and temperatures. $^{15}NO_2^-$ was added as tracer. Box plots show median (black line), 10th, 25th, 75th, and 90th percentiles as vertical boxes with error bars; n = 4–6. White circles show incubations in 0.2-µm-filtered seawater. Rates significantly different from zero are marked with an asterisk; significantly different rates between copepods and ostracods are marked with a double arrow; significantly different rates between water layers are marked with different upper-case (copepods) and lower-case letters (ostracods). n.d., not detected.

to carcass-associated bacteria rather than free-living bacteria in the ambient seawater. However, it cannot be ruled out that (i) carcass-associated bacteria were detaching during the ^{15}N-incubations and remained actively involved in N-cycling as free-living bacteria and (ii) zooplankton carcasses were leaking substrates into the surrounding water and thereby promoted N-cycling by free-living bacteria. In both cases though, significant contributions by free-living bacteria to anaerobic N-cycling would have only been possible under fully anoxic conditions in the incubation bottles.

The rates of the diverse carcass-associated N-cycling pathways showed several clear patterns (**Figure 3**; Table S3): (i) Carcass-associated N-cycling rates were relatively low in the oxic water layer and significantly different from zero only for N_2O production (N_2O-$Prod_{ZP}$) and DNRA activity ($DNRA_{ZP}$) (Table S4), (ii) carcass-associated N-cycling rates were in most cases not different between copepods and ostracods within any given water layer (Table S5), and (iii) the rates of carcass-associated NO_2^--oxidation (NO_2-Ox_{ZP}), NO_3^--reduction (NO_3-Red_{ZP}), N_2O-$Prod_{ZP}$, denitrification (DEN_{ZP}), and anammox (AMX_{ZP}) were highest in the hypoxic/anoxic water layer, while only $DNRA_{ZP}$ rates increased consistently with water depth (Table S6).

In addition to the consumption of the added $^{15}NO_2^-$ tracer (Figures S3b,f,j), high rates of NO_3-Red_{ZP} activity were observed in the hypoxic/anoxic and anoxic water layers (Figures S2f,j). In the hypoxic/anoxic water layer, NO_3-Red_{ZP} scaled with the net production of $NO_{2\ total}^-$ (Figures S2f,g), which suggests high rates of carcass-associated dissimilatory nitrate reduction to nitrite ($DNRN_{ZP}$).

Carcass-associated N_2O production (N_2O-$Prod_{ZP}$) was significantly correlated with $DNRA_{ZP}$ in the oxic water layer, with NO_2-Ox_{ZP} and NO_3-Red_{ZP} in the hypoxic/anoxic water layer, and with DEN_{ZP} in the anoxic water layer (Figure S4, Table S7).

The partitioning between the diverse N-cycling pathways was strikingly different for zooplankton and seawater incubations (**Figure 4**). The relative share of DNRA was without exception larger in zooplankton than in seawater incubations, with the absolute rate and the relative share of $DNRA_{ZP}$ being particularly high in the anoxic water layer. Denitrification was most important in carcasses incubated in seawater from the hypoxic/anoxic layer. The relative share of N_2O-$Prod_{ZP}$ was low in all zooplankton incubations, but N_2O production was dominant in seawater incubations for the hypoxic/anoxic layer. Anammox activity was most important in seawater incubations for the anoxic layer and was not detected in the other two water layers. Only for copepod and ostracod carcasses incubated in seawater from the hypoxic/anoxic layer, a small relative share of AMX_{ZP} was observed.

Direct and Indirect Contribution by Zooplankton Carcasses to Pelagic N-Loss

Zooplankton carcasses may contribute to pelagic N-loss directly by hosting bacteria that produce N_2 and N_2O and indirectly by hosting bacteria that produce NH_4^+ which, together with NH_4^+ released from carcass degradation, may fuel anammox by free-living bacteria. The contribution by zooplankton carcasses to the combined rate of pelagic N_2O production, denitrification, DNRA, and anammox was estimated from the individual-specific N-cycling rates (**Figure 3**) and the *in situ* abundance of copepods and ostracods in GD (**Figure 2C**), assuming a relative carcass abundance of 36%, which corresponds to the mean of minimum and maximum values reported in a recent meta-study (Tang et al., 2014). Due to the dominance of copepods in GD, significant contributions to pelagic N-cycling are almost exclusively linked to this taxonomic group of zooplankton (**Figure 5**). In the oxic water layer, it is in fact only the presence of copepod carcasses, which enables the occurrence of N_2O production, denitrification, DNRA, and anammox, albeit at relatively low rates. In the hypoxic/anoxic water layer though, the estimated N-cycling rates associated with copepod carcasses rival or even exceed those measured in seawater only, while the contribution by ostracod carcasses is small. In contrast, in the anoxic water layer, zooplankton carcasses are estimated to only marginally enhance the rather intense pelagic N-cycling, except for a strong contribution by copepod carcasses to DNRA rates. However, the estimated contribution by zooplankton to pelagic N-loss may actually be higher than observed here, if also live specimens contribute to pelagic N-cycling, e.g., through microbial processes occurring in their anoxic guts.

These contributions by zooplankton carcasses to pelagic N-cycling correspond to or may translate into an enhancement of pelagic N-loss. N_2O-$Prod_{ZP}$, DEN_{ZP}, and AMX_{ZP} correspond to

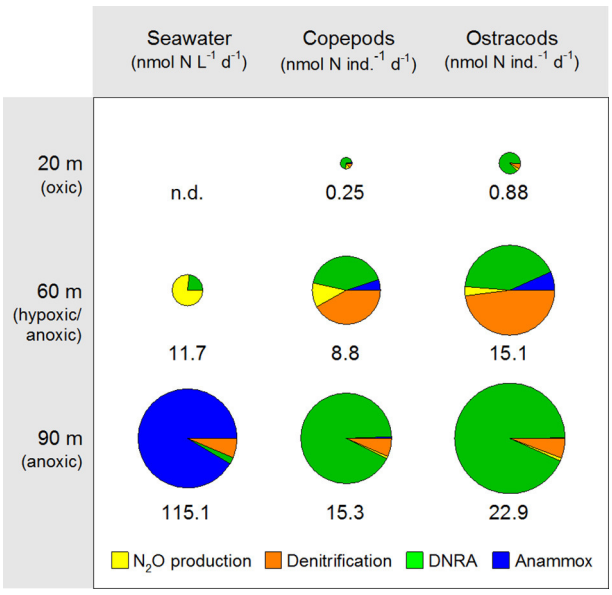

FIGURE 4 | Relative partitioning between N_2O production, denitrification, DNRA, and anammox in zooplankton vs. seawater incubations. Pie chart area is proportional to the lumped rate of N_2O production, denitrification, DNRA, and anammox for any given taxonomic group of zooplankton and water depth. The numerical value of the lumped rate is given below each pie chart. n.d., not detected. Note the different units for zooplankton vs. seawater incubations.

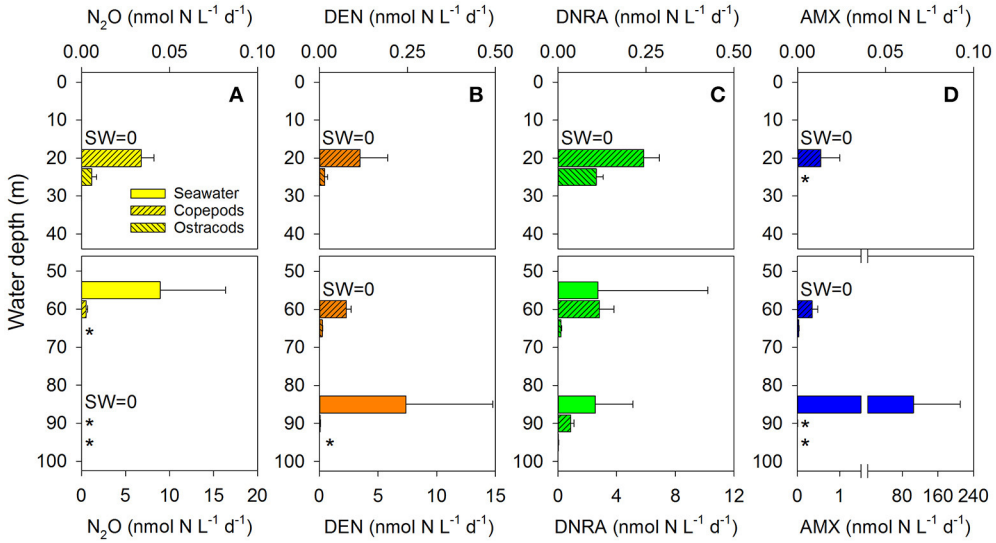

FIGURE 5 | Extrapolated N-cycling rates associated with zooplankton carcasses. Individual-specific rates of **(A)** N_2O production, **(B)** denitrification (DEN), **(C)** DNRA, and **(D)** anammox (AMX) presented in **Figure 3** were extrapolated to the *in situ* abundance of copepods and ostracods presented in **Figure 2C** and assuming a relative carcass abundance of 36% (Tang et al., 2014). N-cycling rates measured in seawater incubations are shown for comparison. Each panel is split into an upper and a lower part to account for the low rates measured in the oxic water layer. Means and standard error of 4–6 replicate measurements are shown. SW = 0 indicates rates in seawater incubations not significantly different from zero; * indicates rates in zooplankton incubations lower than 0.02 nmol N L^{-1} d^{-1}.

N-loss in all water layers, while $DNRA_{ZP}$ and carcass degradation might contribute to N-loss only in the anoxic water layer by fueling free-living anammox bacteria with NH_4^+. The most pronounced enhancement of pelagic N-loss is estimated to occur in the hypoxic/anoxic water layer where zooplankton abundance is still relatively high and pelagic N-loss proceeds solely through ambient N_2O production, but not denitrification and anammox. Here, carcass-associated N-cycling is estimated to increase pelagic N-loss by a factor as high as 1.4 (**Table 1**). In the anoxic water layer, however, carcass-associated N-cycling is estimated to increase the intense pelagic N-loss by a factor of 1.02 only. For the oxic water layer, pelagic N-loss was not detected in seawater incubations and therefore it is not possible to calculate an enhancement factor for the anyway low carcass-mediated N-loss.

In the anoxic water layer, $NH_4^+{}_{total}$ production (NH_4-$Prod_{ZP}$) due to carcass degradation and $DNRA_{ZP}$ was on average 1.9-fold higher than NH_4^+ production by $DNRA_{ZP}$ alone (Figures S2l, S5a). This multiplication factor further increases the estimates given in **Figure 5C** and is already accounted for in **Table 1**. The degradation-related origin of this $NH_4^+{}_{total}$ is confirmed by the significant correlation between NH_4-$Prod_{ZP}$ and O_2-$Cons_{ZP}$, which suggests C/N ratios of organic matter degradation of 9.2 (Figure S5b). This value is similar to the C/N ratios calculated for the biomass of the copepod and ostracod carcasses (see above). Notably, in the hypoxic/anoxic water layer, a net uptake of $NH_4^+{}_{total}$ by zooplankton carcasses was observed (Figure S2h), even though the high O_2-$Cons_{ZP}$ rates (Figure S2e) would suggest high NH_4-$Prod_{ZP}$ rates due to carcass degradation. This net uptake of $NH_4^+{}_{total}$ by zooplankton carcasses is most likely due to intense N-assimilation by rapidly growing bacteria associated with the carcasses, as indicated by a 2- to 5-fold increase of O_2-$Cons_{ZP}$ rates during the 8-h incubation period, which was not observed in either of the other water layers (data not shown).

TABLE 1 | Depth-integrated rates of pelagic N-loss.

Depth interval (m)	N-loss (μmol N m^{-2} d^{-1})		
	Seawater	Zooplankton carcasses (direct contribution)	Zooplankton carcasses (direct + indirect contribution)
0–40	0	7.4 ± 3.2	7.4 ± 3.2
40–70	268 ± 223	104 ± 14	104 ± 14
70–100	3377 ± 3164	2.4 ± 1.2	74 ± 18
Total	3645 ± 3172	114 ± 14	186 ± 23

*Depth-integrated rates of pelagic N-loss (mean ± standard error) were calculated as the sum of volumetric rates of N_2O production, denitrification, and anammox measured in seawater incubations multiplied with the thickness of the respective depth interval. The contribution by zooplankton carcasses to pelagic N-loss was estimated for a relative carcass abundance of 36% (Tang et al., 2014), using data presented in **Figure 5**. The direct contribution by carcasses comprises N_2O-$Prod_{ZP}$, DEN_{ZP}, and AMX_{ZP}, whereas the direct + indirect contribution comprises N_2O-$Prod_{ZP}$, DEN_{ZP}, AMX_{ZP}, and NH_4-$Prod_{ZP}$ (incl. $DNRA_{ZP}$).*

DISCUSSION

Carcass-Associated N-Loss in the Presence of Oxygen

The ^{15}N-incubation experiments conducted under different environmental conditions imply that the relative enhancement of pelagic N-loss by zooplankton carcasses is greatest in oxic

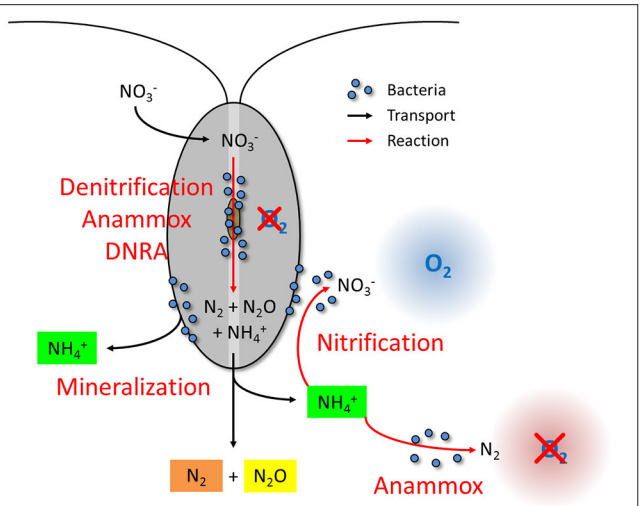

FIGURE 6 | Conceptual scheme of zooplankton-carcass-associated N-cycling and potential effects on pelagic N-cycling. Microbial N-cycling may take place in the anoxic interior and on the exoskeleton of zooplankton carcasses. Anaerobic N-cycling associated with zooplankton carcasses contributes to pelagic N-loss both directly via N_2 and N_2O production (through denitrification and anammox) and indirectly via NH_4^+ production (through DNRA and mineralization) that may fuel free-living anammox bacteria in anoxic water layers. Carcass-derived NH_4^+ may also fuel microbial nitrification in oxic and hypoxic water layers.

and hypoxic water layers. In the presence of O_2, the N-loss mediated by free-living bacteria is generally very limited. At ambient O_2 levels higher than 1–20 μmol L^{-1}, denitrification and anammox activities by free-living bacteria are usually inhibited (Kalvelage et al., 2011; Dalsgaard et al., 2014) and bacterial or archaeal nitrifiers contribute to N-loss only marginally through N_2O production (Frame and Casciotti, 2010; Löscher et al., 2012). Thus, under oxic and hypoxic conditions, zooplankton carcasses must act as (partially) anoxic pelagic hotspots that host microbial N-cycling pathways which directly contribute to N-loss, namely N_2O production, denitrification, and anammox (**Figure 6**).

In the oxic water layer, N-loss via N_2O and N_2 production was exclusively enabled by the presence of copepod and ostracod carcasses because the corresponding background rates in seawater were not significantly different from zero. The individual-specific N_2O and N_2 production rates were very low though and added up to only ∼0.25 nmol N L^{-1} d^{-1}, despite the high abundance of copepods and ostracods in this water layer. In comparison, the N-loss rate measured in seawater incubations for the anoxic layer was >100 nmol N L^{-1} d^{-1}, which was similar to the N-loss rate measured in anoxic bottom water of GD in an earlier study (Dalsgaard et al., 2003).

In the hypoxic/anoxic water layer, individual-specific N_2O and N_2 production rates were 1–2 orders of magnitude higher than in the oxic layer. These increased rates are likely explained by the expansion of the anoxic volume inside the carcasses due to the lowered ambient O_2 level as previously shown for sinking diatom and cyanobacterial aggregates (Klawonn et al., 2015; Stief et al., 2016; Lundgaard et al., 2017) and large copepod carcasses (Glud et al., 2015). Additionally, the occurrence of short anoxic phases during the incubation period may have boosted anaerobic N-cycling. It can also not be ruled out that the higher individual-specific N-cycling rates are linked to differences in the bacterial community composition between the oxic and the hypoxic/anoxic water layer.

Taking the relatively high copepod and ostracod abundances in the hypoxic/anoxic water layer into account, the extrapolated carcass-associated N-loss was here 14-fold higher than in the oxic water layer. Strikingly, the presence of carcasses is estimated to increase pelagic N-loss 1.4-fold in this water layer where the background rates in seawater already reached ∼10% of the N-loss in the anoxic water layer. In the hypoxic/anoxic water layer, pelagic N-loss proceeded exclusively through N_2O rather than N_2 production, which is commonly observed in low-oxygen aquatic environments: N_2O yields of nitrification and denitrification are often high at low ambient O_2 levels (Goreau et al., 1980; Bonin and Raymond, 1990), while N_2 production via denitrification and anammox may be completely inhibited above low-micromolar levels of O_2 (Kalvelage et al., 2011; Dalsgaard et al., 2014). It needs to be noted though that the seawater incubations did not reach anoxic conditions and thus the rates of anaerobic N-cycling may be underestimated relative to the zooplankton incubations.

In the presence of O_2, carcass-associated N-loss proceeded mainly through DEN_{ZP} and to a smaller extent through N_2O-$Prod_{ZP}$ and AMX_{ZP}. Elevated rates of DEN_{ZP} at lower ambient O_2 levels have previously been reported for carcasses of the copepod *C. finmarchicus* (Glud et al., 2015) that has a much larger prosome length (∼2,600 μm) than *Oncaea* sp. and *Oithona* sp. (<500 μm). Apparently, reduced ambient O_2 levels turn the copepod carcasses into more and more O_2-depleted microsites enhancing the potential for anaerobic N-cycling. In the current study, the DEN_{ZP} rate measured for copepod carcasses under hypoxic/anoxic conditions (0–100 μmol O_2 L^{-1}) and at 21.5°C amounted to 3.3 nmol N $individual^{-1}$ d^{-1}. The much larger *C. finmarchicus* carcasses reached the same rate at ∼10 μmol O_2 L^{-1} and at 7°C (Glud et al., 2015). Moreover, the DEN_{ZP} rate of *C. finmarchicus* carcasses increased exponentially to >50 nmol N $individual^{-1}$ d^{-1} at 1 μmol O_2 L^{-1} (Glud et al., 2015).

Carcass-associated N-loss is also mediated by N_2O-$Prod_{ZP}$, albeit at lower rates than by DEN_{ZP}. The origin of the N_2O produced by zooplankton carcasses remains unresolved because only N_2O_{total} was measured. The most prominent sources of N_2O are nitrification (strictly speaking: ammonia oxidation) and denitrification. Nitrous oxide production associated with larger invertebrates has been ascribed to both nitrification and denitrification (Svenningsen et al., 2012; Heisterkamp et al., 2013). As in their benthic counterparts, the live copepods and ostracods may host denitrification activity in their anoxic gut and nitrification activity on their exoskeleton. Both processes may also be involved in N_2O production by carcasses, provided that these possess an anoxic interior and an oxic body surface. Indeed, N_2O-$Prod_{ZP}$ was significantly correlated with both NO_2-Ox_{ZP} and NO_3-Red_{ZP} in the

hypoxic/anoxic water layer, which is compatible with both NO_3^--producing and NO_3^--consuming pathways as possible sources of N_2O.

Carcass-associated anammox activity was detected in the hypoxic/anoxic water layer, but not in the anoxic water layer. This is surprising given the pronounced O_2 sensitivity of anammox bacteria and also because a prevalence of anammox bacteria as colonizers of the carcasses would rather be expected in the anoxic water layer. However, anammox bacteria were also identified and anammox activity was detected in a sponge that hosts both oxic and anoxic microenvironments (Hoffmann et al., 2009).

In the hypoxic/anoxic water layer, high rates of $DNRN_{ZP}$ might be inferred from the co-occurring NO_3^- consumption and NO_2^- production at an almost equimolar ratio. Nitrite produced by $DNRN_{ZP}$ may theoretically fuel the anammox process (De Brabandere et al., 2014), which was not detected in seawater incubations for this water layer though.

The estimated 1.4-fold enhancement of N-loss by zooplankton carcasses in the hypoxic/anoxic water layer is based on a relative carcass abundance of 36% and on only about half of the total community of mesozooplankton in GD. Additionally, it can be assumed that also live specimens of copepods and ostracods host anaerobic N-cycling pathways, the rates of which still need to be quantified though. Thus, the 1.4-fold enhancement of N-loss represents a relatively conservative estimate. Irrespective of the exact extent of carcass-associated N-loss at high ambient O_2 levels, it is likely to be overlooked in studies that address N-loss in OMZs. First, pre-filtration of seawater for rate measurements will remove the carcasses; second, if non-filtered seawater is used, only a sparse number of incubation vials will contain a single carcass; third, oxic and hypoxic water layers are often excluded from sampling schemes because N-loss mediated by free-living bacteria is not expected to occur in the presence of O_2.

Carcass-Associated N-Loss in the Absence of Oxygen

Under fully anoxic conditions, DNRA was clearly the dominant N-cycling pathway associated with zooplankton carcasses. Also under oxic and hypoxic conditions, $DNRA_{ZP}$ rates were high compared to DEN_{ZP}, AMX_{ZP}, and $N_2O\text{-}Prod_{ZP}$ rates. The crucial difference between $DNRA_{ZP}$ proceeding in the presence or absence of O_2 is that exclusively in the anoxic bottom water of GD, the carcass-derived NH_4^+ might fuel the activity of free-living anammox bacteria. It may thus be speculated that zooplankton carcasses sinking through the anoxic bottom water may contribute to N-loss to a large extent indirectly. This mechanism seems plausible for GD because NH_4^+ concentrations were below 50 nmol L^{-1} in the anoxic, non-sulfidic water layer at the time of the current study (Laura A. Bristow, pers. comm.). Additionally, it has been shown that the *in situ* anammox activity in GD can be stimulated by experimental NH_4^+ addition (Dalsgaard et al., 2003). Ammonium produced by $DNRA_{ZP}$ adds to the NH_4^+ excreted by live zooplankton or produced by the degradation of carcasses and fecal pellets (**Figure 6**). Our results indicate that for the copepods and ostracods in GD, $DNRA_{ZP}$ approximately doubles the rate of NH_4^+ production due to carcass degradation and thus significantly enforces the potential indirect contribution to pelagic N-loss.

It has previously been suggested that migrating zooplankton supplies NH_4^+ to the anammox process in OMZs (Bianchi et al., 2014). The underlying mechanism is known as "active transport" of substrates and nutrients by migrating zooplankton (Steinberg et al., 2000; Schnetzer and Steinberg, 2002). Organic matter export to depth is thought to be more efficiently mediated by migrating zooplankton that congregate at the boundary or within OMZs during daytime than by sinking organic aggregates that are rapidly degraded already during their descent (Kalvelage et al., 2013; Bianchi et al., 2014). However, NH_4^+ excretion by live zooplankton may be down-regulated due to anoxic conditions (Kiko et al., 2016). Our findings demonstrate though that NH_4^+ release by zooplankton is also due to carcass degradation and carcass-associated DNRA activity, in particular if specimens die close to their daytime migration depth. Notably, $DNRA_{ZP}$ rates were highest under anoxic conditions where NH_4^+ excretion by live specimens may be particularly low.

The carcasses might be preferentially colonized by DNRA bacteria that were residing in the gut of the live specimens. Anoxia and high availability of organic carbon relative to NO_3^- in the gut of invertebrates may favor DNRA over denitrification (Giblin et al., 2013). Interestingly, many of the bacterial groups recurring in the different copepod microbiomes (i.e., Bacteroidetes, Firmicutes, Actinobacteria, *Vibrio* sp.) comprise representatives that colonize the gut of other animals and also possess *nrf*, the key gene for the DNRA process (Mohan et al., 2004; Welsh et al., 2014; Decleyre et al., 2015).

An estimate for the anoxic bottom water in GD indicates that the extrapolated rate of $NH_4\text{-}Prod_{ZP}$ (incl. $DNRA_{ZP}$) is ~2-fold higher than the DNRA rate measured in seawater. This additional NH_4^+ supplied by carcasses corresponds to 6.3% of the anammox rate measured in seawater (105 nmol N L^{-1} d^{-1}). Rates of denitrification and N_2O production in seawater and zooplankton incubations were insignificant compared to the DNRA rates and thus the zooplankton carcasses potentially enhance N-loss in the anoxic water layer only marginally.

Ecological Implications

Integrated over the top 100 m of the stratified water column of GD, zooplankton carcasses potentially enhance N-loss between 1.03-fold (considering direct contributions through N_2 and N_2O production) and 1.05-fold (considering direct and indirect contributions through N_2, N_2O, and NH_4^+ production). The largest fraction of direct contributions is to be expected in the hypoxic/anoxic water layer (1.4-fold increase), while indirect contributions come into play in the anoxic water layer only and are still minor compared to background rates in the ambient water (1.02-fold increase). Thus, zooplankton carcasses have mainly the potential to functionally extend the anoxic volume of OMZs at their hypoxic boundaries. The low levels of ambient O_2 in these zones allow relatively high zooplankton abundances and very high individual-specific N-cycling rates, but efficiently inhibit pelagic N-loss through anaerobic N-cycling processes mediated by free-living bacteria.

However, the vertical extent of the oxycline in GD is relatively small (∼20 m) compared to the thickness of the anoxic bottom water where the bulk of pelagic N-loss is mediated by free-living bacteria (∼100 m). Therefore, the significant contribution by zooplankton carcasses to pelagic N-loss in the hypoxic/anoxic water layer does not translate into a major enhancement of depth-integrated N-loss in GD. In contrast, open-ocean OMZs possess upper and lower hypoxic boundaries spanning depth intervals of several hundreds of meters and regularly host high zooplankton abundances (Wishner et al., 2013; Hirche et al., 2014). In such settings, the relative contribution by zooplankton carcasses to depth-integrated N-loss is likely much larger than observed in GD. The relative carcass abundance in zooplankton in and around OMZs has to our knowledge not been investigated so far. It may be assumed that relative carcass abundance increases with decreasing ambient O_2 level due to non-predatory mortality. In that case, the contributions by carcasses to pelagic N-cycling will gain additional importance in the hypoxic and anoxic zones of the OMZs.

The functional extension of the anoxic volume of OMZs has previously been proposed to be mediated by sinking diatom aggregates (Kamp et al., 2016; Stief et al., 2016; Lundgaard et al., 2017), but may as well be caused by other pelagic microbial hotspots with an anoxic center, such as sinking cyanobacterial aggregates, live specimens of zooplankton, and fecal pellets (Tang et al., 2011; Glud et al., 2015; Klawonn et al., 2015). Globally, OMZs are projected to expand significantly within the next century due to climate change (Stramma et al., 2008; Keeling et al., 2010). Thus, anaerobic N-cycling inside pelagic microbial hotspots will most likely intensify and increase the N-loss from the ocean, aside from any possible negative feedbacks (Kalvelage et al., 2011).

The contribution by zooplankton carcasses to N-loss through N_2 production might be counteracted by carcass-associated N_2 fixation activity. However, individual-specific N_2 production rates measured in the current study were at least three orders of magnitude higher than N_2 fixation rates measured for small copepods in another study (Scavotto et al., 2015). Despite the possible variability of N-cycling associated with mesozooplankton from different habitats, this large difference in rates suggests that carcass-associated microbial communities exhibit net consumption rather than net production of fixed nitrogen in the pelagic zone.

Copepods and ostracods are by far not the only groups of zooplankton that may host anaerobic N-cycle activities. In GD, other zooplankton species might also be of importance as colonization sites for N-cycle bacteria and as potentially anoxic microsites. The gastropod *Cuvierina* sp. reached very high abundances in GD during the time of the current study and might host microbial biofilms involved in N-cycling on their shell (Heisterkamp et al., 2013). In freshwater ecosystems, copepods and daphnids are abundant and may qualify as pelagic microbial hotspots (Tang et al., 2009). The large *Calanus* species need more attention regarding the diverse N-cycle processes they may host besides denitrification (Glud et al., 2015). In the global ocean, krill and copepods compete for the status as the most abundant multi-cellular animals on Earth. Due to their large body size, krill most likely possess anoxic guts and might thus also represent anoxic pelagic microsites, despite high ambient O_2 levels in their natural habitat. Establishing the pathways and magnitude of N-cycle activities associated with these abundant groups of zooplankton will allow first estimates of their quantitative contribution to pelagic N-cycling in the global ocean.

AUTHOR CONTRIBUTIONS

PS and RG designed the study. PS, AL, AM, and BT carried out sample collection, incubation experiments, sample analysis, and data analysis. PS wrote the manuscript with input from all co-authors.

FUNDING

This study was financially supported by the Danish National Research Council (grant no. 0602-02276B), the European Research Council (HADES, grant no. 669947; OXYGEN, grant no. 267233), and the University of Southern Denmark.

ACKNOWLEDGMENTS

We would like to thank Morten Larsen for providing the CTD data. Eleazar Ruíz Campos, Eddy Gomez Ramírez, Emilio Garcia-Robledo, and Laura A. Bristow are acknowledged for their technical help during the field campaign. Rie Pors, Dina Holmgård Skov, Susanne Møller, and Carolina Sheridan Rodríguez are acknowledged for sample analyses.

SUPPLEMENTARY MATERIAL

The Supplementary Material for this article can be found online at: http://journal.frontiersin.org/article/10.3389/fmars.2017.00152/full#supplementary-material

REFERENCES

Bianchi, D., Babbin, A. R., and Galbraith, E. D. (2014). Enhancement of anammox by the excretion of diel vertical migrators. *Proc. Natl. Acad. Sci. U.S.A.* 111, 15653–15658. doi: 10.1073/pnas.1410790111

Bickel, S. L., Tang, K. W., and Grossart, H. P. (2009). Use of aniline blue to distinguish live and dead crustacean zooplankton composition in freshwaters. *Freshwater Biol.* 54, 971–981. doi: 10.1111/j.1365-2427.2008.02141.x

Bonin, P., and Raymond, N. (1990). Effects of oxygen on denitrification in marine sediments. *Hydrobiologia* 207, 115–122. doi: 10.1007/BF00041447

Bower, C. E., and Holm-Hansen, T. (1980). A salicylate-hypochlorite method for determining ammonia in seawater. *Can. J. Fish. Aquat. Sci.* 37, 794–798. doi: 10.1139/f80-106

Dalsgaard, T., Canfield, D. E., Petersen, J., Thamdrup, B., and Acuna-Gonzalez, J. (2003). N_2 production by the anammox reaction in the anoxic water column of Golfo Dulce, Costa Rica. *Nature* 422, 606–608. doi: 10.1038/nature01526

Dalsgaard, T., Stewart, F. J., Thamdrup, B., De Brabrandere, L., Revsbech, N. P., Ulloa, O., et al. (2014). Oxygen at nanomolar levels reversibly suppresses process rates and gene expression in anammox and denitrification in the oxygen minimum zone off Northern Chile. *mBio* 5:e01966–14. doi: 10.1128/mBio.01966-14

Dalsgaard, T., Thamdrup, B., Farias, L., and Revsbech, N. P. (2012). Anammox and denitrification in the oxygen minimum zone of the eastern South Pacific. *Limnol. Oceanogr.* 57, 1331–1346. doi: 10.4319/lo.2012.57.5.1331

De Brabandere, L., Canfield, D. E., Dalsgaard, T., Friederich, G. E., Revsbech, N. P., Ulloa, O., et al. (2014). Vertical partitioning of nitrogen-loss processes across the oxic-anoxic interface of an oceanic oxygen minimum zone. *Environ. Microbiol.* 16, 3041–3054. doi: 10.1111/1462-2920.12255

Decleyre, H., Heylen, K., Van Colen, K., and Willems, A. (2015). Dissimilatory nitrogen reduction in intertidal sediments of a temperate estuary, small-scale heterogeneity and novel nitrate-to-ammonium reducers. *Front. Microbiol.* 6:1124. doi: 10.3389/fmicb.2015.01124

De Corte, D., Lekunberri, I., Sintes, E., Garcia, J. A. L., Gonzales, S., and Herndl, G. J. (2014). Linkage between copepods and bacteria in the North Atlantic Ocean. *Aquat. Microb. Ecol.* 72, 215–225. doi: 10.3354/ame01696

DeVries, T., Deutsch, C., Rafter, P. A., and Primeau, F.,(2013). Marine denitrification rates determined from a global 3-D inverse model. *Biogeosciences* 10, 2481–2496. doi: 10.5194/bg-10-2481-2013

Dubilier, N., Mulders, C., Ferdelman, T., de Beer, D., Pernthaler, A., Klein, M., et al. (2001). Endosymbiotic sulphate-reducing and sulphide-oxidizing bacteria in an oligochaete worm. *Nature* 411, 298–302. doi: 10.1038/35077067

Elliott, D. T., and Tang, K. W. (2009). Simple staining method for differentiating live and dead marine zooplankton in field samples. *Limnol. Oceanogr. Methods* 7, 585–594. doi: 10.4319/lom.2009.7.585

Escribano, R., Hidalgo, P., and Krautz, C. (2009). Zooplankton associated with the oxygen minimum zone system in the northern upwelling region of Chile during March 2000. *Deep Sea Res. II* 56, 1049–1060. doi: 10.1016/j.dsr2.2008.09.009

Ferdelman, T. G., Thamdrup, B., Canfield, D. E., Glud, R. N., Kuever, J., Lillebaek, R., et al. (2006). Biogeochemical controls on the oxygen, nitrogen and sulfur distributions in the water column of Golfo Dulce, an anoxic basin on the Pacific coast of Costa Rica revisited. *Rev. Biol. Trop.* 54, 171–191. doi: 10.15517/rbt.v54i1.26825

Frame, C. H., and Casciotti, K. L. (2010). Biogeochemical controls and isotopic signatures of nitrous oxide production by a marine ammonia-oxidizing bacterium. *Biogeosciences* 7, 2695–2709. doi: 10.5194/bg-7-2695-2010

Füssel, J., Lam, P., Lavik, G., Jensen, M. M., Holtappels, M., Gunter, M., et al. (2012). Nitrite oxidation in the Namibian oxygen minimum zone. *ISME J.* 6, 1200–1209. doi: 10.1038/ismej.2011.178

Garcia-Robledo, E., Corzo, A., and Papaspyrou, S. (2014). A fast and direct spectrophotometric method for the sequential determination of nitrate and nitrite at low concentrations in small volumes. *Mar. Chem.* 162, 30–36. doi: 10.1016/j.marchem.2014.03.002

Gerdts, G., Brandt, P., Kreisel, K., Boersma, M., Schoo, K. L., and Wichels, A. (2013). The microbiome of North Sea copepods. *Helgoland Mar. Res.* 67, 757–773. doi: 10.1007/s10152-013-0361-4

Giblin, A. E., Tobias, C. R., Song, B., Weston, N., Banta, G. T., and Rivera-Monroy, V. H. (2013). The importance of dissimilatory nitrate reduction to ammonium (DNRA) in the nitrogen cycle of coastal ecosystems. *Oceanography* 26, 124–131. doi: 10.5670/oceanog.2013.54

Glud, R. N., Grossart, H. P., Larsen, M., Tang, K. W., Arendt, K. E., Rysgaard, S., et al. (2015). Copepod carcasses as microbial hot spots for pelagic denitrification. *Limnol. Oceanogr.* 60, 2026–2036. doi: 10.1002/lno.10149

Goreau, T. J., Kaplan, W. A., Wofsy, S. C., McElroy, M. B., Wimbis, F. W., and Watson, S. W. (1980). Production of NO_2^- and N_2O by nitrifying bacteria at reduced concentrations of oxygen. *Appl. Environ. Microbiol.* 40, 526–532.

Heisterkamp, I. M., Schramm, A., Larsen, L. H., Svenningsen, N. B., Lavik, G., de Beer, D., et al. (2013). Shell biofilm-associated nitrous oxide production in marine molluscs, processes, precursors and relative importance. *Environ. Microbiol.* 15, 1943–1955. doi: 10.1111/j.1462-2920.2012.02823.x

Hirche, H. J., Barz, K., Ayon, P., and Schulz, J. (2014). High resolution vertical distribution of the copepod *Calanus chilensis* in relation to the shallow oxygen minimum zone off northern Peru using LOKI, a new plankton imaging system. *Deep Sea Res. I* 88, 63–73. doi: 10.1016/j.dsr.2014.03.001

Hoffmann, F., Radax, R., Woebken, D., Holtappels, M., Lavik, G., Rapp, H. T., et al. (2009). Complex nitrogen cycling in the sponge *Geodia barretti*. *Environ. Microbiol.* 11, 2228–2243. doi: 10.1111/j.1462-2920.2009.01944.x

Kalvelage, T., Jensen, M. M., Contreras, S., Revsbech, N. P., Lam, P., Günter, M., et al. (2011). Oxygen sensitivity of anammox and coupled N-cycle processes in Oxygen Minimum Zones. *PLoS ONE* 6:e29299. doi: 10.1371/journal.pone.0029299

Kalvelage, T., Lavik, G., Lam, P., Contreras, S., Arteaga, L., Loescher, C. R., et al. (2013). Nitrogen cycling driven by organic matter export in the South Pacific oxygen minimum zone. *Nat. Geosci.* 6, 228–234. doi: 10.1038/ngeo1739

Kamp, A., Stief, P., Bristow, L. A., Thamdrup, B., and Glud, R. N. (2016), Intracellular nitrate of marine diatoms as a driver of anaerobic nitrogen cycling in sinking aggregates. *Front. Microbiol.* 7:1669. doi: 10.3389/fmicb.2016.01669

Keeling, R. F., Körtzinger, A., and Gruber, N. (2010). Ocean deoxygenation in a warming world. *Ann. Rev. Mar. Sci.* 2, 199–299. doi: 10.1146/annurev.marine.010908.163855

Kiko, R., Hauss, H., Buchholz, F., and Melzner, F. (2016). Ammonium excretion and oxygen respiration of tropical copepods and euphausiids exposed to oxygen minimum zone conditions. *Biogeosciences* 13, 2241–2255. doi: 10.5194/bg-13-2241-2016

Kirillin, G., Grossart, H. P., and Tang, K. W. (2012). Modeling sinking rate of zooplankton carcasses: effects of stratification and mixing. *Limnol. Oceanogr.* 57, 881–894. doi: 10.4319/lo.2012.57.3.0881

Klawonn, I., Bonaglia, S., Brüchert, V., and Ploug, H. (2015). Aerobic and anaerobic nitrogen transformation processes in N_2-fixing cyanobacterial aggregates. *ISME J.* 9, 1456–1466. doi: 10.1038/ismej.2014.232

Löscher, C. R., Kock, A., Könneke, M., LaRoche, J., Bange, H. W., and Schmitz, R. A. (2012). Production of oceanic nitrous oxide by ammonia-oxidizing archaea. *Biogeosciences* 9, 2419–2429. doi: 10.5194/bg-9-2419-2012

Lundgaard, A. S. B., Treusch, A. H., Stief, P., Thamdrup, B., and Glud, R. N. (2017). Nitrogen cycling and bacterial community structure of sinking and aging diatom aggregates. *Aquat. Microb. Ecol.* 79, 85–99.

Martinez-Garcia, M., Stief, P., Diaz-Valdes, M., Wanner, G., Ramos-Espla, A., Dubilier, N., et al. (2008). Ammonia-oxidizing Crenarchaeota and nitrification inside the tissue of a colonial ascidian. *Environ. Microbiol.* 10, 2991–3001. doi: 10.1111/j.1462-2920.2008.01761.x

McIlvin, M. R., and Altabet, M. A. (2005). Chemical conversion of nitrate and nitrite to nitrous oxide for nitrogen and oxygen isotopic analysis in freshwater and seawater. *Anal. Chem.* 77, 5589–5595. doi: 10.1021/ac050528s

Mohan, S. B., Schmid, M., Jetten, M., and Cole, J. (2004). Detection and widespread distribution of the *nrfA* gene encoding nitrite reduction to ammonia, a short circuit in the biological nitrogen cycle that competes with denitrification. *FEMS Microbiol. Ecol.* 49, 433–443. doi: 10.1016/j.femsec.2004.04.012

Moisander, P. H., Sexton, A. D., and Daley, M. C. (2015). Stable associations masked by temporal variability in the marine copepod microbiome. *PLoS ONE* 10:e0138967. doi: 10.1371/journal.pone.0138967

Møller, E. F., Riemann, L., and Søndergaard, M. (2007). Bacteria associated with copepods, abundance, activity and community composition. *Aquat. Microb. Ecol.* 47, 99–106. doi: 10.3354/ame047099

Morales-Ramírez, Á., Acuña-González, J., Lizano, O., Alfaro, E., and Gómez, E. (2015). Rasgos oceanográficos en el Golfo Dulce, Pacífico de Costa Rica: una revisión para la toma de decisiones en conservación marina. *Rev. Biol. Trop.* 63, 131–160.

Nielsen, L. P. (1992). Denitrification in sediment determined from nitrogen isotope pairing. *FEMS Microbiol. Ecol.* 86, 357–362. doi: 10.1111/j.1574-6968.1992.tb04828.x

Nuester, J., Shema, S., Vermont, A., Fields, D. M., and Twining, B. S. (2014). The regeneration of highly bioavailable iron by meso- and microzooplankton. *Limnol. Oceanogr.* 59, 1399–1409. doi: 10.4319/lo.2014.59.4.1399

Padilla, C. C., Bertagnolli, C. A., Bristow, L. A., Sarode, N., Glass, J. B., Thamdrup, B., et al. (2017). Metagenomic binning recovers a transcriptionally active gamma-proteobacterium linking methanotrophy to partial denitrification in an anoxic oxygen minimum zone. *Front. Mar. Sci.* 4:23. doi: 10.3389/fmars.2017.00023

Parris, D. J., Ganesh, S., Edgcomb, V. P., DeLong, E. F., and Stewart, F. J. (2014). Microbial eukaryote diversity in the marine oxygen minimum zone off northern Chile. *Front. Microbiol.* 5:543. doi: 10.3389/fmicb.2014.00543

Plante, C. J., and Jumars, P. (1992). The microbial environment of marine deposit-feeder guts characterized via microelectrodes. *Microb. Ecol.* 23, 257–277. doi: 10.1007/BF00164100

Ploug, H., Kühl, M., Buchholz-Cleven, B., and Jørgensen, B. B. (1997). Anoxic aggregates - an ephemeral phenomenon in the pelagic environment? *Aquat. Microb. Ecol.* 13, 285–294. doi: 10.3354/ame013285

Revsbech, N. P. (1989). An oxygen microsensor with a guard cathode. *Limnol. Oceanogr.* 34, 474–478. doi: 10.4319/lo.1989.34.2.0474

Saba, G. K., Steinberg, D. K., and Bronk, D. A. (2011). The relative importance of sloppy feeding, excretion, and fecal pellet leaching in the release of dissolved carbon and nitrogen by *Acartia tonsa* copepods. *J. Exp. Mar. Biol. Ecol.* 404, 47–56. doi: 10.1016/j.jembe.2011.04.013

Scavotto, R. E., Dziallas, C., Bentzon-Tilia, M., Riemann, L., and Moisander, P. H. (2015). Nitrogen-fixing bacteria associated with copepods in coastal waters of the North Atlantic Ocean. *Environ. Microbiol.* 17, 3754–3765. doi: 10.1111/1462-2920.12777

Schnetzer, A., and Steinberg, D. K. (2002). Active transport of particulate organic carbon and nitrogen by vertically migrating zooplankton in the Sargasso Sea. *Mar. Ecol. Prog. Ser.* 234, 71–84. doi: 10.3354/meps234071

Shoemaker, K. M., and Moisander, P. H. (2015). Microbial diversity associated with copepods in the North Atlantic subtropical gyre. *FEMS Microbiol. Ecol.* 91:fiv064. doi: 10.1093/femsec/fiv064

Skovgaard, A., Castro-Mejia, J. L., Hansen, L. H., and Nielsen, D. S. (2015). Host-specific and pH-dependent microbiomes of copepods in an extensive rearing system. *PLoS ONE* 10:e0132516. doi: 10.1371/journal.pone.0132516

Song, G. D., Liu, S. M., Marchant, H., Kuypers, M. M. M., and Lavik, G. (2013). Anammox, denitrification and dissimilatory nitrate reduction to ammonium in the East China Sea sediment. *Biogeosciences* 10, 6851–6864. doi: 10.5194/bg-10-6851-2013

Steinberg, D. K., Goldthwait, S. A., and Hansell, D. A. (2000). Zooplankton vertical migration and the active transport of dissolved organic and inorganic nitrogen in the Sargasso Sea. *Deep Sea Res. I* 49, 1445–1461. doi: 10.1016/S0967-0637(02)00037-7

Stief, P., and Eller, G. (2006). The gut microenvironment of sediment-dwelling *Chironomus plumosus* larvae as characterised with O_2, pH, and redox microsensors. *J. Comp. Physiol. B* 176, 673–683. doi: 10.1007/s00360-006-0090-y

Stief, P., Kamp, A., Thamdrup, B., and Glud, R. N. (2016). Anaerobic nitrogen turnover by sinking diatom aggregates at varying ambient oxygen levels. *Front. Microbiol.* 7:98. doi: 10.3389/fmicb.2016.00098

Stief, P., Poulsen, M., Nielsen, L. P., Brix, H., and Schramm, A. (2009). Nitrous oxide emission by aquatic macrofauna. *Proc. Natl. Acad. Sci. U.S.A.* 106, 4296–4300. doi: 10.1073/pnas.0808228106

Stramma, L., Johnson, G. C., Sprintall, J., and Mohrholz, V. (2008). Expanding oxygen-minimum zones in the tropical oceans. *Science* 320, 655–658. doi: 10.1126/science.1153847

Svenningsen, N. B., Heisterkamp, I. M., Sigby-Clausen, M., Larsen, L. H., Nielsen, L. P., Stief, P., et al. (2012). Shell biofilm nitrification and gut denitrification contribute to emission of nitrous oxide by the invasive freshwater mussel *Dreissena polymorpha* (*Zebra mussel*). *Appl. Environ. Microbiol.* 78, 4505–4509. doi: 10.1128/AEM.00401-12

Tang, K. W. (2005). Copepods as microbial hotspots in the ocean: effects of host feeding activities on attached bacteria. *Aquat. Microb. Ecol.* 38, 31–40. doi: 10.3354/ame038031

Tang, K. W., Bickel, S. L., Dziallas, C., and Grossart, H. P. (2009). Microbial activities accompanying decomposition of cladoceran and copepod carcasses under different environmental conditions. *Aquat. Microb. Ecol.* 57, 89–100. doi: 10.3354/ame01331

Tang, K. W., Gladyshev, M. I., Dubovskaya, O. P., Kirillin, G., and Grossart, H. P. (2014). Zooplankton carcasses and non-predatory mortality in freshwater and inland sea environments. *J. Plankton Res.* 36, 597–612. doi: 10.1093/plankt/fbu014

Tang, K. W., Glud, R. N., Glud, A., Rysgaard, S., and Nielsen, T. G. (2011). Copepod guts as biogeochemical hotspots in the sea: evidence from microelectrode profiling of *Calanus* spp. *Limnol. Oceanogr.* 56, 666–672. doi: 10.4319/lo.2011.56.2.0666

Tang, K. W., Hutalle, K. M. L., and Grossart, H. P. (2006). Microbial abundance, composition and enzymatic activity during decomposition of copepod carcasses. *Aquat. Microb. Ecol.* 45, 219–227. doi: 10.3354/ame045219

Tang, K. W., Turk, V., and Grossart, H. P. (2010). Linkage between crustacean zooplankton and aquatic bacteria. *Aquat. Microb. Ecol.* 61, 261–277. doi: 10.3354/ame01424

Teuber, L., Schukat, A., Hagen, W., and Auel, H. (2013). Distribution and ecophysiology of calanoid copepods in relation to the Oxygen Minimum Zone in the Eastern Tropical Atlantic. *PLoS ONE* 8:e775590. doi: 10.1371/journal.pone.0077590

Thamdrup, B., Canfield, D. E., Ferdelman, T. G., Glud, R. N., and Gundersen, J. K. (1996). A biogeochemical survey of the anoxic basin Golfo Dulce, Costa Rica. *Rev. Biol. Trop.* 44, 19–33.

Thamdrup, B., and Dalsgaard, T. (2002). Production of N_2 through anaerobic ammonium oxidation coupled to nitrate reduction in marine sediments. *Appl. Environ. Microbiol.* 68, 1312–1318. doi: 10.1128/AEM.68.3.1312-1318.2002

Warembourg, F. R. (1993). "Nitrogen fixation in soil and plant systems," in *Nitrogen Isotope Techniques,* eds R. Knowles and T. H. Blackburn (New York, NY: Academic Press). 157–180.

Welsh, A., Chee-Sanford, J. C., Connor, L. M., Löffler, F. E., and Sanford, R. A. (2014). Refined NrfA phylogeny improves PCR-based *nrfA* gene detection. *Appl. Environ. Microbiol.* 80, 2110–2119. doi: 10.1128/AEM.03443-13

Wishner, K. F., Outram, D. M., Seibel, B. A., Daly, K. L., and Williams, R. L. (2013). Zooplankton in the eastern tropical north Pacific: boundary effects of oxygen minimum zone expansion. *Deep Sea Res. I* 79, 122–140. doi: 10.1016/j.dsr.2013.05.012

Zehr, J. P., Mellon, M. T., and Zani, S. (1998). New nitrogen-fixing microorganisms detected in oligotrophic oceans by amplification of nitrogenase (*nifH*) genes. *Appl. Environ. Microbiol.* 64, 3444–3450.

Conflict of Interest Statement: The authors declare that the research was conducted in the absence of any commercial or financial relationships that could be construed as a potential conflict of interest.